83-1922

TRANSONIC FLOW CALCULATIONS USING TRIANGULAR FINITE ELEMENTS

Richard B. Pelz and Antony Jameson
Princeton University, Princeton, NJ

ABSTRACT

This paper desribes a technique for finding the numerical solution of the Full Potential equation for steady transonic flow about airfoils. The exterior but finite domain is discretized by breaking it up into triangles. Difference equations are formulated using variational principle and a formula for the derivative in an arbitrary polygon. The iterative schemes include multigrid-ADI for structured grids and modified checkerboard for more arbitrary grids. Results show consistency and compare favorably with codes using quadrilateral elements.

INTRODUCTION

Solutions to the potential flow equation have been shown to give accurate predictions of the aerodynamic characteristics of streamlined bodies in the low transonic speed range. Computer codes that solve numerically for the potential flow about wings and airfoils, coupled with a boundary layer correction algorithm, provide crucial design and analysis tools for efficient shapes in the new generation of commercial aircraft.

For a single airfoil in an external domain, fast and reliable methods exist to generate a grid and to solve the resulting difference equations. Now the task before the computational aerodynamicist is to develop techniques to find the solution over more complicated geometries such as multi-element airfoils.

The Augmentor Airfoil(1), for example, is an asymmetric airfoil with two aft auxiliary foils originally designed for STOL purposes. It has been shown experimentally to have surprisingly low drag, and efficient manuevering characteristics at transonic speeds. Whether these characteristics are due to viscous effects or are a property of the inviscid flow is a question which may be answered through analysis of the potential flow about such a configuration.

In obtaining the difference equation, the two best known ways that are suited for handling complex geometries are the finite element and finite volume methods(2,3). The mapping function from the computational to the physical domain used to transform the equations in the finite difference method is not needed for the finite volume method because the difference equation is formulated in the physical plane. In finite element theory the governing differential equation is replaced by a variational principle and solution methods can be applied directly in the physical plane.

The most commonly used element to date has been the quadrilateral with bilinear variation of the potential and isoparametric representation. However, the triangular finite element has some interesting advantages. First, the triangle is the simplest two-dimensional geometric figure with area; thus one would think grid generation around complex geometries might be easier than with quadrilaterals. For example, the discretization of an n-element airfoil and far field boundary produces an n+1 connected domain with a polygonal boundary. It can be proved that both triangle and quadrilateral finite elements can cover this domain exactly, but triangulation might be done in a more efficient manner.

Secondly, if one restricts the potential to vary linearly between vertices of a triangle, then the gradient (the velocity) is constant within the triangle. Hence there is no error associated with integration of the variational, since the integrand is a function only of the velocity. The difference equation reduces to a simple formula that can be thought of as a mass flux balance on a secondary polygonal cell around the node. The Retarded Density/Artificial Compressibility method is used to modify the difference scheme in order to enforce the entropy condition.

The more complex the geometry, the harder it is to create grids which have structure, i.e., which have each grid line being parameterized with a variable varying in a monotonically increasing fashion. The existing methods, patching, conformal mapping, solving nonlinear elliptic equations, and integral curve methods(4), all have difficulties in generating efficient curvilinear coordinate systems around n-element airfoils. Inevitably the aspect ratio of some elements becomes large, which leads to inaccuracies.

On the other hand, one can fit a completely unstructured grid of fairly low aspect ratio elements about almost any domain. One of the authors is currently developing an algorithm to cover a domain with triangles that have strict bounds on their aspect ratio. The use of an unstructured grid restricts the choice of the iterative scheme. Point schemes are the only alternative, unless one wants to invert directly the full sparse but unstructured matrix and use a Newton type iteration.

Depending on the structure, one of two iterative schemes were used on triangular grids. A multilevel iterative scheme was constructed based on the checkerboard scheme for unstructured grids. A fast iterative method, Multigrid-ADI, was used on the structured grids.

This paper discusses the derivation of the difference scheme on triangles, and tries to establish its accuracy and usefulness in computing the transonic flow around airfoils.

DERIVATION OF DIFFERENCE EQUATIONS

Suppose one must estimate df/dx in an arbitrary polygon with n-1 sides and values of f given at each of the n nodes. Define the average value of df/dx as the area integral over the polygon,

$$\overline{\frac{\partial f}{\partial x}} = \frac{1}{A} \iint \frac{\partial f}{\partial x}\, dx\, dy \qquad (1)$$

where A is the area of the polygon. Using Green's theorem, the expression becomes

$$\overline{\frac{\partial f}{\partial x}} = \frac{1}{A} \oint f\, dy, \qquad (2)$$

and taking a representative value of f for a edge to be the average of the end-point values, one finds

$$\overline{\frac{\partial f}{\partial x}} = \frac{1}{A} \sum_{k=1}^{N} \frac{f_{k+1} + f_k}{2} (y_{k+1} - y_k). \qquad (3)$$

The index N+1 is 1. The same procedure gives an exact equation for the area,

$$A = \iint dx\, dy = \oint x\, dy = \sum_{k=1}^{N} \frac{x_{k+1} + x_k}{2} (y_{k+1} - y_k). \qquad (4)$$

Restricting one's attention to triangles, define the velocity potential as the function defined at the nodes; assume further that the potential varies linearly between nodes. The polygon formula derived above gives exact expressions for the velocities u and v. Since three points determine a plane, the trial function in a triangle is an equation for a plane, and the gradient will be constant within the triangle, see figure 1A.

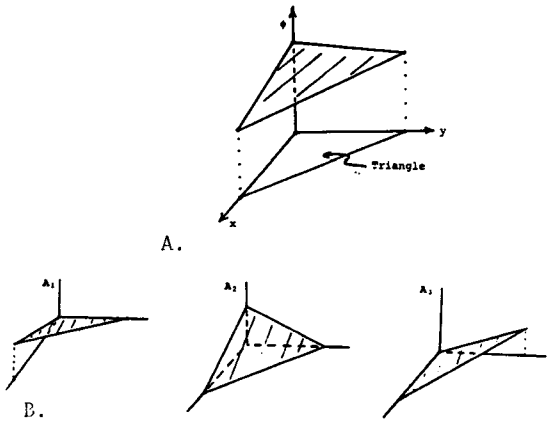

Figure 1. A. Trial function
B. Basis functions

This representation of the potential is analogous to the Area Basis Functions of Finite Element Theory(5), see figure 1B. The trial function is

$$\phi = \phi_1 A_1 + \phi_2 A_2 + \phi_3 A_3 \qquad (5)$$

where

$$A_1 = \frac{x(y_3-y_2)+x_2(y-y_3)+x_3(y_2-y)}{x_1(y_3-y_2)+x_2(y_1-y_3)+x_3(y_2-y_1)}$$

$$A_2 = \frac{x_1(y_3-y)+x(y_1-y_3)+x_3(y-y_1)}{x_1(y_3-y_2)+x_2(y_1-y_3)+x_3(y_2-y_1)} \qquad (6)$$

$$A_3 = \frac{x_1(y-y_2)+x_2(y_1-y)+x(y_2-y_1)}{x_1(y_3-y_2)+x_2(y_1-y_3)+x_3(y_2-y_1)}.$$

For a difference scheme to be compatible, the potential must be continuous between elements. Compatibility is ensured in triangles by the linearity of the potential; no isoparametric representation is needed.

The variational principle for compressible, inviscid, irrotational flow was desribed by Bateman(6). Consider the integral

$$I = \iint P(\nabla\phi)\, dx\, dy \qquad (7)$$

where P is given by the isentropic relation

$$P = \frac{1}{\gamma M_\infty^2} \rho^\gamma, \qquad (8)$$

$$\rho = \left[1 + \frac{\gamma-1}{2} M_\infty^2 (1-\nabla\phi\cdot\nabla\phi)\right]^{\frac{1}{\gamma-1}}.$$

The solution ϕ of the continuity equation for a compressible, inviscid, irrotational flow is a stationary point of the integral. This can be seen by noting that the Euler-Lagrange equation of I is the continuity equation, since

$$\frac{\partial P}{\partial u} = -\rho u \quad \text{and} \quad \frac{\partial P}{\partial v} = -\rho v . \tag{9}$$

The integral can be cast as the sum of integrals over the N triangles that make up the domain,

$$I = \sum_{i=1}^{N} \iint P \, dx \, dy . \tag{10}$$

Because of the constant gradient, the pressure is constant in each triangle; thus

$$I = \sum_{i=1}^{N} P_i A_i . \tag{11}$$

Taking the first variation, one finds

$$\delta I = \sum_{i=1}^{N} [(\frac{\partial P}{\partial u})_i \delta u_i + (\frac{\partial P}{\partial v})_i \delta v_i] A_i . \tag{12}$$

From the polygon formula $(\delta u, \delta v)_i$ can be written

$$(\delta \nabla \phi)_i = (\frac{\partial \nabla \phi}{\partial \phi_1}\delta\phi_1 + \frac{\partial \nabla \phi}{\partial \phi_2}\delta\phi_2 + \frac{\partial \nabla \phi}{\partial \phi_3}\delta\phi_3)_i$$

$$= \frac{1}{2A_i}[(y_2-y_3)(x_3-x_2)\delta\phi_1 \tag{13}$$

$$+(y_3-y_1)(x_1-x_3)\delta\phi_2+(y_1-y_2)(x_2-x_1)\delta\phi_3]_i$$

where the subscripts 1,2 and 3 refer to the three vertices of the ith triangle.

Reordering in terms of the points j = 1,2,...,M, the expression for the first variational becomes

$$\delta I = -\sum_{j=1}^{M} S_j \delta\phi_j \tag{14}$$

where

$$S_j = \frac{1}{2}\sum_{k=1}^{6} \rho_k (u_k \Delta y_k - v_k \Delta x_k) \tag{15}$$

and where j is the index for the center point and k is the index of the surrounding six triangles, Δx and Δy are the lengths of the leg opposite the jth node, see figure 2.

The discrete Euler-Lagrange equation is

$$S_j = 0 \tag{16}$$

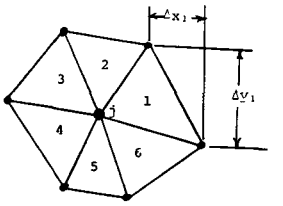

Figure 2. Difference formula stencil

at every point j, j=1,2,...,M.

Physically,

$$\frac{1}{2}\rho(u\Delta y - v\Delta x) \tag{17}$$

is a mass flux through some surface in the jth triangle. A representative surface is the one drawn dotted in figure 3A, the endpoints being the midpoints of two legs extending from the jth node. Since the density and velocity are constant, the surface that extends through the midcell point is equally as representative, figure 3B. the midcell point, figure 3B. Thus S approximates a mass flux in a secondary cell formed from the mid-cell points. The secondary mesh is interlocking, thus the domain is completely covered once, figure 4A.

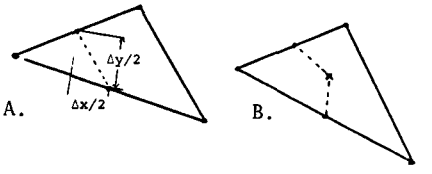

Figure 3. Flux line and modification

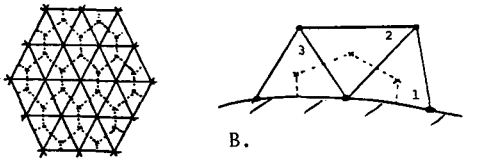

Figure 4. A. Secondary cell, B. boundary

Consider the six-triangle group pictured in figure 5A; for Laplace's equation the flux balance formula becomes just the discrete Laplacian,

$$S_j = \frac{1}{\Delta x^2}(\phi_1 - 2\phi_0 + \phi_4) + \frac{1}{\Delta y^2}(\phi_2 - 2\phi_0 + \phi_5) . \tag{18}$$

Consider further the group in figure 5B; the flux balance equation for Laplace's equation is

$$\Delta^2 S_j = (\phi_1 - 2\phi_0 + \phi_4) + (\phi_2 - 2\phi_0 + \phi_5) + (\phi_3 - 2\phi_0 + \phi_6) . \tag{19}$$

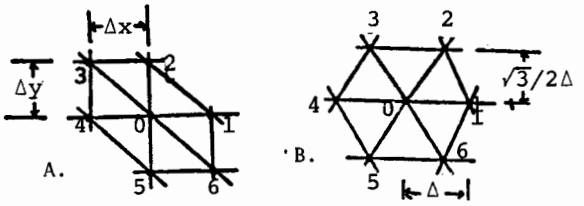

Figure 5. A.,B. Polygon examples

This equation is logical if one appeals to the Mean Value Theorem for harmonic functions.

The boundary conditions are

$$\phi \rightarrow \frac{1}{2\pi} \tan^{-1} \left(\sqrt{1 - M_\infty^2}\, \frac{Y}{X}\right) \quad \text{as } x,y \rightarrow \infty \tag{20}$$

in the far field ,and

$$\frac{\partial \phi}{\partial n} = 0 \tag{21}$$

on the airfoil. The difference equation for points on the airfoil involves only three triangles. The mass flux balance still holds, however, with just the three, figure 4B.

For the solution to be unique, the Kutta condition, that the flow leave the trailing edge smoothly, must be enforced. A branch cut, across which there is a constant jump in potential from the airfoil to the outer boundary, is also nessecary if a bound vortex is contained in the airfoil. Since there are actually two values of the potential at a point on the cut, there must be two conditions there. One is

$$\phi^+ - \phi^- = \Gamma = \text{const along cut,} \tag{22}$$

and the other is that the flux balance hold. In the special case of the trailing edge point, the flux balance from the upper secondary cell will give the flux into the lower secondary cell and vice versa, thus giving two conditions.

In supercritical flows, nonuniqueness can be caused by expansion shocks, which can appear as a result of ignoring the second law of Thermodynamics. A biasing of the difference scheme upstream provides a way to exclude the non-physical solutions. The addition of the proper upwind bias is accomplished by moving the point of evaluation of the densities slightly upstream. This method of retarding the densities was developed by Eberle(7) and Hafez et al(8).

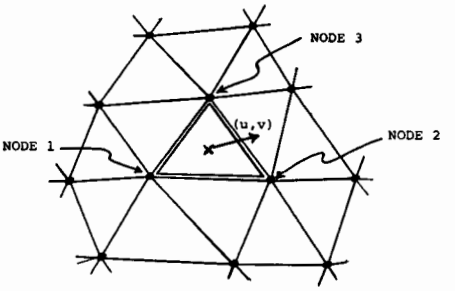

Figure 6. Retarded density diagram

The quantity

$$\frac{\partial \rho}{\partial s} = \left(\frac{\partial \rho}{\partial x} u + \frac{\partial \rho}{\partial y} v\right)/q \tag{23}$$

is evaluated at nodes if the averaged Mach number is greater than some cutoff number, $M_c \leq 1$. The quantity (23) is calculated using the polygon formula on the polygon formed by the secondary cell. The density of a triangle is then modified by locating the node that is nearest to the upstream direction from the triangle centroid, node 1 of figure 6, and

$$\tilde{\rho} = \rho - \delta \left(\mu \frac{\partial \rho}{\partial s}\right)_1 \tag{24}$$

where δ is the distance between the centroid and node 1 and where

$$\mu_1 = \text{Max}\,(1 - M_c^2/M^2, 0). \tag{25}$$

The modified densities replace the regular densities in the flux balance formula. This procedure makes for a fully rotated scheme, however, it lowers by one the order of accuracy.

GRID GENERATION

Two types of triangular grids were used to test the difference equations: a structured grid produced by placing diagonals on a quadrilateral grid, and an unstructured grid produced by an algebraic method.

The quadrilateral grid is generated by an airfoil-to-slit transformation, which produces an H-type grid. A square root transformation maps the input airfoil and slit computational domain to upper half planes. The mapped airfoil coordinates are then added to the computational plane by a shearing map. The physical plane is generated using a square map on the sheared plane. There is a sparseness of points around the leading edge that is corrected by a

nonorthogonal map in the intermediate plane. For more details, see Pelz(9); the resulting grid is shown in figure 7.

The algebraic algorithm was originally developed by Bank(10), and is still being modified for n-element airfoil grids by one of the authors. Basically it takes a simply connected

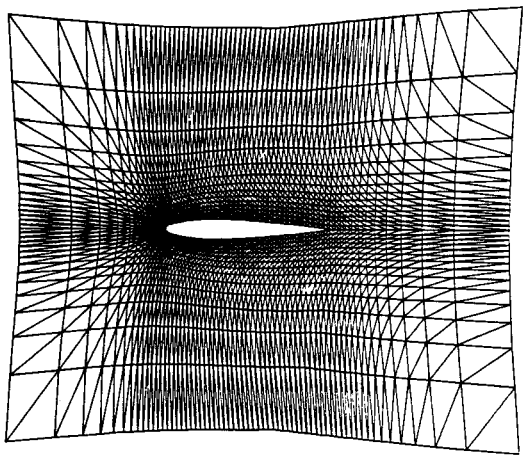

Figure 7. Structured grid NACA 0012 64 x 32

domain, and searches the boundary to find three adjacent points that satisfy the criterion

$$4\sqrt{3}A/(h_1^2+h_2^2+h_3^2) \geq \beta \qquad (26)$$

where A is the area and the h's are the distances between the points. For high quality triangles, β = .5 gives an aspect ratio of less than 13/4 for isoceles triangles.

If the resulting domain is still a many-sided polygon, it is split into two domains and the searching is done on both domains. This procedure continues until the domain is completely covered. One typical result is shown in figure 8. An advantage of the method is that one has control in the placement of triangles.

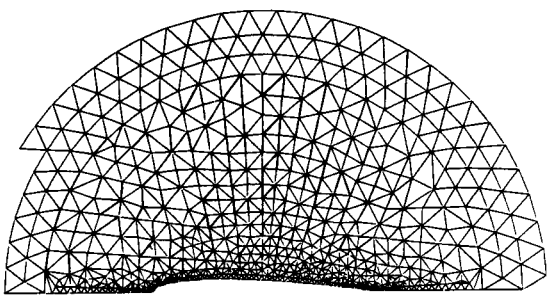

Figure 8. Unstructured grid NACA 0012 128 points on airfoil

ITERATIVE SCHEME

On the structured grid rapid convergence was obtained using a multigrid method adapted for transonic flow problems by Jameson(11). The linear differential equation

$$L[\phi] = f \qquad (27)$$

can be approximated on a grid of mesh size h by

$$L^h[\phi^h] = f^h. \qquad (28)$$

Letting the initial guess be ϕ_0^h, there exists a correction $\delta\phi^h$ such that

$$L^h[\phi_0^h + \delta\phi^h] = f^h. \qquad (29)$$

Instead of solving for the correction on the grid of mesh size h, one solves for it on a grid of mesh size 2h,

$$L^{2h}[\delta\phi^{2h}] = I_h^{2h}\{f^h - L^h[\phi_0^h]\} \qquad (30)$$

where I is an operator transferring the values from the h grid to the 2h grid. The fine grid residual becomes the forcing function for the coarse grid problem. Using the same procedure, the problem can be cast on the 4h grid.

To transfer the correction from the coarse to fine grid, an interpolation operator is defined,

$$\phi_1^h = I_{2h}^h \delta\phi_0^{2h} + \phi_0^h. \qquad (31)$$

At each step a smoothing operator is used to damp the errors caused by the transfer.

In this way the signal propagation per iteration is increased to the width of the largest grid, and the errors in each frequency band are damped on an appropriate grid. This method is extended to nonlinear problems by using the full approximation scheme of Brandt(12),

$$L^{2h}[\phi_1^{2h}] = I_h^{2h}\{f^h - L^h[\phi_0^h]\} + L^{2h}[\phi_0^{2h}]$$
$$\phi_1^h = \phi_0^h + I_{2h}^h\{\phi_1^{2h} - \phi_0^{2h}\}. \qquad (32)$$

The algorithm to damp the high frequency errors (aliased on coarser grids) at each multigrid step is a generalization of the Alternating Direction scheme

of Peaceman and Rathford(13). The left side of the correction-residual equation

$$\alpha N \delta\phi^n = -\omega L(\phi^n) \qquad (33)$$

is factored in a way approximating L,

$$\alpha N = (\alpha - A\delta_x^2)(\alpha - B\delta_y^2) \qquad (34)$$

where

$$A \sim \rho(1 - u^2/a^2) \ , \ B \sim \rho(1 - v^2/a^2),$$

ω is the relaxation parameter, and α is a parameter to be chosen.

Since the above equation yields a parabolic equation in psuedotime, the parameter α is replaced by the operator

$$\alpha = \alpha_0 + \alpha_1 \delta_x^- + \alpha_2 \delta_y^- , \qquad (35)$$

giving a hyperbolic equation necessary in supersonic flow. The choice of $\alpha_1, \alpha_2, \alpha_3$ is made to keep the proper domain of dependence.

For unstructured grids where neighboring points can be considered to be independent of each other, a point scheme is necessary. Since successive schemes require updated neighboring nodes, the Jacobi scheme is the only scheme possible.

Consider the two-step Jacobi scheme called the checkerboard scheme,

$$a(\delta\phi^{n+1} - \delta\phi^n) + b\delta\phi^n = \omega L(\phi^{n+1}) \qquad (36)$$

where

$$\delta\phi^n = \phi^{n+1} - \phi^n.$$

It requires the same order operations to obtain a converged solution as point SOR, which is a considerable gain over single step Jacobi.

Consider further a modification of the checkerboard scheme to supersonic flow by the addition of a streamwise derivative of the correction(14). To analyze this, the time analogy is used on the quasilinear equation,

$$\alpha\phi_{tt} + \beta\phi_{st} = -(M^2 - 1)\phi_{ss} + \phi_{nn}. \qquad (37)$$

Letting

$$T = t - \frac{\beta}{2(M^2 - 1)} , \qquad (38)$$

$$S = s \ , \ N = n$$

gives

$$[\alpha - \frac{\beta^2}{4(M^2 - 1)}]\phi_{TT} = -(M^2 - 1)\phi_{SS} + \phi_{NN}. \qquad (39)$$

Requiring S to be the timelike direction restricts

$$\beta > 2\sqrt{\alpha(M^2 - 1)}. \qquad (40)$$

The modification is realized on triangles by

$$\alpha(\delta\phi^{n+1} - \delta\phi^n) + \beta\Delta s \frac{\partial(\delta\phi^n)}{\partial s} = \omega L(\phi^{n+1}). \qquad (41)$$

The second term on the left can be calculated by the polygon formula for the derivative in the triangle directly upstream of the node in question.

RESULTS

Tests were performed for a single NACA 0012 airfoil in a domain which extends 3-5 chords from the airfoil. Results for structured grids are shown in figures 9 to 12. Figure 9 shows a Cp distribution at M=.5, alpha=0. No discernible difference was found in comparing this solution to a quadrilateral finite volume code of Jameson (FLO42).

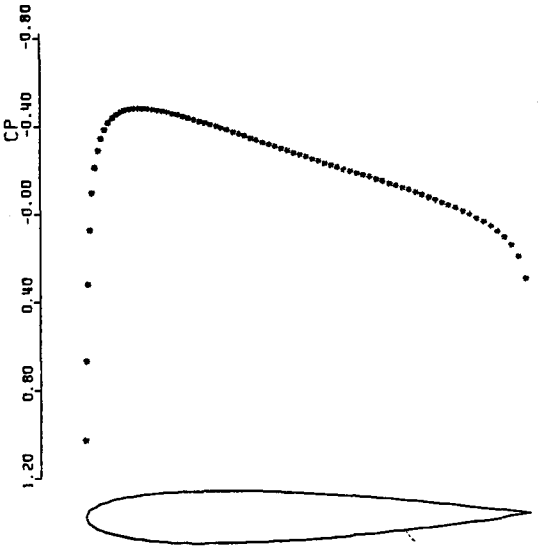

Figure 9. Subcritical pressure distribution

Figure 10 shows a series of supercritical runs with decreasing mesh size. The change in the solutions decreases progressively, implying that as the mesh size goes to zero, the solution is that of the original PDE. Figure 11 shows a plot of drag coefficient against mesh size squared. The straight line indicates second-order accuracy. The formulation of the difference equations using triangles results in a conservative, apparently second-order scheme for transonic cases. Figure 12 gives a comparison with FL042 on grids with comparible number of nodes. The shock is somewhat sharper in the triangle case, mainly because the H-grid has more points in that region than the O-type grid of FL042.

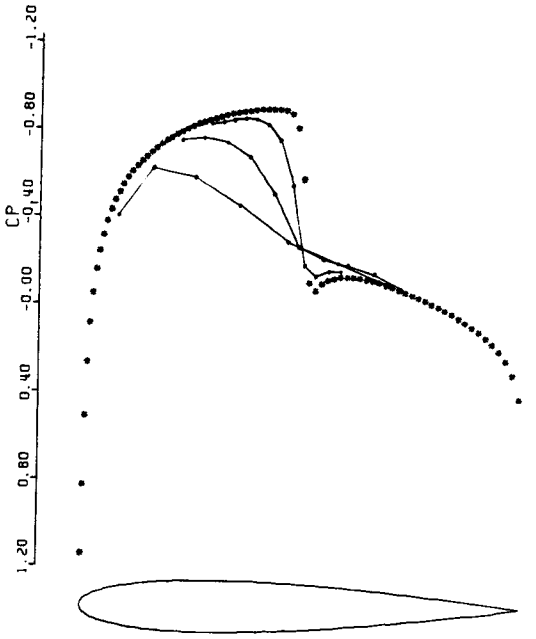

NACA 0012
MACH 0.800 ALPHA 0.0
CL 0.0000 CD 0.0069 CM -0.0000
GRID 128X 64 NCYC 100 RES 0.93D-07

Figure 10. Convergence plot
grids 16x8, 32x16, 64x32, 128x64

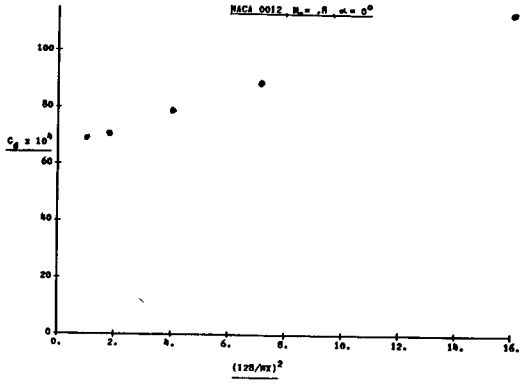

Figure 11. Plot of drag versus mesh size

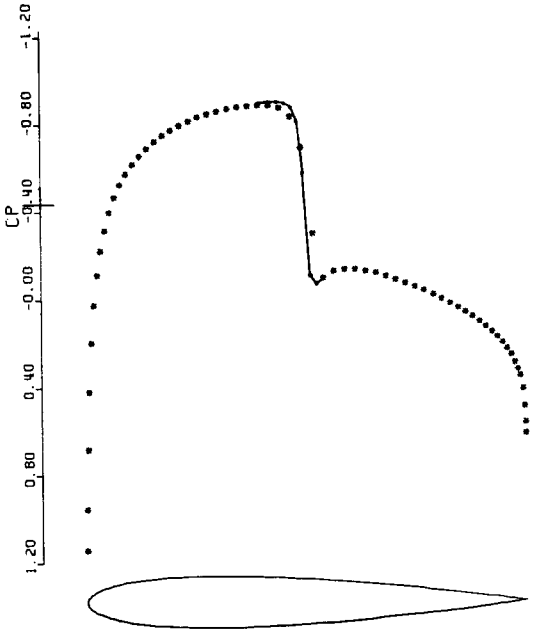

NACA 0012
MACH 0.800 ALPHA 0.0
CL 0.0000 CD 0.0059 CM 0.0000
GRID 128X32 NCYC 20 RES0.613D-07

Figure 12. Pressure distribution for supercritical case
* FL042, -- triangle code

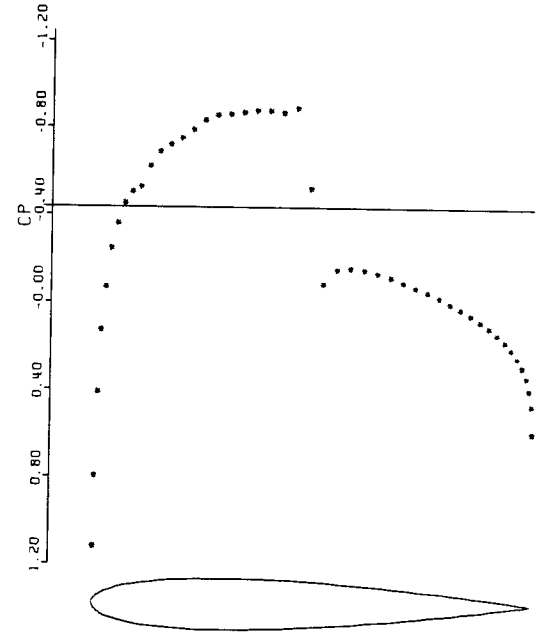

NACA 0012 FL047
MACH 0.800 ALPHA 0.0
CL -0.0000 CD 0.0066 CM 0.0000
ELEMENT 1/1 NCYC 1001 RES 0.36D-07

Figure 13. Pressure distribution for supercritical case on unstructured grid

Figure 13 shows a result for an unstructured grid. Globally, it compares well with Figure 12; however, the wiggles in the supersonic zone are caused by either the varying of triangle areas, or insufficient resolution near the airfoil.

REFERENCES

[1] Farbridge, J.E. and Smith, R.C., 'The Transonic Multi-Foil Augmentor-Wing', AIAA Paper 77-606.

[2] Habashi, W.G. and Hafez, M.M., 'Finite Element Solution of Transonic Problems', AIAA paper 81-1472.

[3] Jameson, A. and Caughey, D.A., 'A Finite Volume Method of Transonic Potential Flow Calulations', AIAA 77-635.

[4] Thompson,J.F., 'A Survey of Grid Generation Techniques in Computational Fluid Dynamics, AIAA paper 83-447.

[5] Lapidus, Leon and Pinder, George F., Numerical Solution of Partial Differential Equations in Science and Engineering, Wiley, New York (1982).

[6] Bateman, H., 'Notes on a Differential Equation which occurs in Two Dimensional Motion of a Compressible Fluid and the Associated Variational Problems', Roy. Soc. Proc., vol 121, p 194 (1928).

[7] Eberle,A., 'Eine Method Finiter Elements Berechnungder Transsonicken PotentialStrimung un Profile', MMB Berich Nr. UFE 1352(0) (1977).

[8] Hafez, M., South, J., and Murman, E., 'Artificial Compressibility for Numerical Solutions of Transonic Full Potential Equation', AIAA paper 78-1149.

[9] Pelz, R.B., Steinhoff,J.S., 'Multigrid-ADI Solution of the Transonic Full Potential Equation for Airfoils Mapped to Slits', Proceedings from ASME Winter Meeting November 1981.

[10] Bank, R.E., 'PLTMG User's Guide, Technical Report, Dept of Mathematics, UCSD, June 1981

[11] Jameson, A., 'Acceleration of Transonic Potential Flow Calculations on Arbitrary Meshes by the Multiple Grid Method', AIAA Paper 79-1458.

[12] Brandt, A, 'Multi-level adaptive solution to boundary value problems', Math. Comp., Vol. 31, 1977, pp 333-391.

[13] Peaceman,D.W., Rathford,H.H., 'The numerical solution of parabolic and elliptic differential equations', SIAM Journal Vol. 3, 1955, pp 28-41.

[14] Keller, J.D., Jameson, A., 'Preliminary Study of the Use of the STAR-100 Computer for Transonic Flow Calculations', NASA TM 74086, November 1977.

—END